AD NUMBER
AD352684
CLASSIFICATION CHANGES
TO: unclassified
FROM: secret
LIMITATION CHANGES
TO: Approved for public release, distribution unlimited
FROM: Distribution authorized to DoD and DoD contractors only; Administrative/Operational Use; 20 AUG 1964. Other requests shall be referred to Defense Atomic Support Agency, Washington, DC 20301.
AUTHORITY
DNA ltr, 14 Sep 1995; DNA ltr, 14 Sep 1995

DISCLAIMER NOTICE

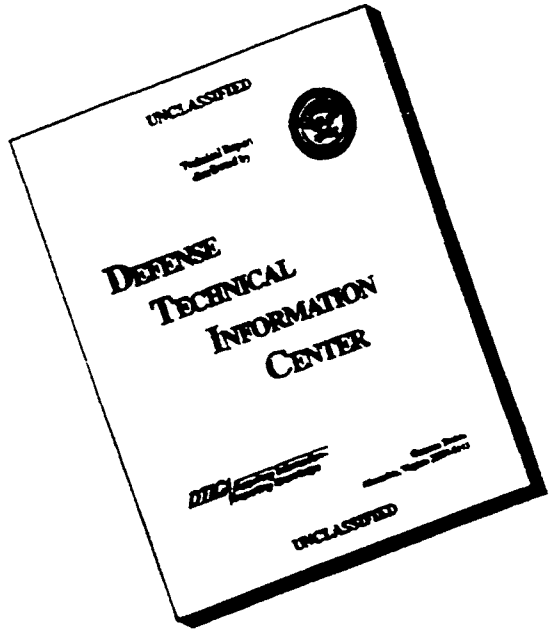

THIS DOCUMENT IS BEST QUALITY AVAILABLE. THE COPY FURNISHED TO DTIC CONTAINED A SIGNIFICANT NUMBER OF PAGES WHICH DO NOT REPRODUCE LEGIBLY.

[redacted]

POR-2011
(WT-2011)

This document consists of 49 pages
No. 156 of 372 copies, Series A

Operation

DOMINIC

CHRISTMAS SERIES

PROJECT OFFICERS REPORT—PROJECT 1.2

SHOCK PHOTOGRAPHY (U)

P. Hanlon, Project Officer

U.S. Naval Ordnance Laboratory
White Oak, Silver Spring, Md.

[redacted]

Issuance Date: August [illegible] 1964

[redacted]

[redacted]

Inquiries relative to this report may be made to

Chief, Defense Atomic Support Agency
Washington, D. C. 20301

When no longer required, this document may be destroyed in accordance with applicable security regulations.

DO NOT RETURN THIS DOCUMENT

[redacted]

[redacted]

[redacted]

POR-2011
(WT-2011)

OPERATION DOMINIC

CHRISTMAS SERIES

PROJECT OFFICERS REPORT — PROJECT 1.2

SHOCK PHOTOGRAPHY (U)

P. H[illegible]don, Project Officer

U. S. Naval Ordnance Laboratory
White Oak, Silver Spring, Md.

[redacted]

[redacted]

ABSTRACT

The objectives of Project 1.2, "Shock Photography," were:

(a) To augment the data available for the free-air pressure-distance curve, and to investigate the effects of large yields and varying altitudes on scaling.

(b) To obtain basic radius-time data in a non-homogeneous atmosphere in order to investigate the effects of a real atmosphere on air shocks resulting from free-air shots.

In addition to the required data, shock radius-time data were obtained along the surface, and radius-time data of a cool inner zone within the shock sphere were measured.

All the data were derived from films obtained by Edgerton, Germeshausen and Grier, Inc.

Based solely on the agreement of the scaled radius-time and pressure-distance data of Shots Bighorn, Priscilla and Diablo with the standard free-air curves, the empirical free-air curves appear to be valid for use with yields up to ~ 10 Mt and heights of burst up to ~ 12,000 feet. [redacted]

A comparison of the horizontal (homogeneous atmosphere) and vertical (non-homogeneous atmosphere) shock arrival time data indicated that the rate of vertical shock growth was greater than that of the horizontal. However, the validity of these velocity differences is very doubtful because of the great scatter in the vertical data. Conclusions are not warranted.

[redacted]

Based upon the surface radium-time data of Bighorn and Sunset, and the overpressure distance data in the Mach region obtained from Bighorn, the near-ideal height of burst curves could be used within the stipulated reliability limits.

[redacted]

PREFACE

Project 1.2, "Shock Photography," had a dual role on Operation Dominic.

For the Fish Bowl series this project was established initially to cooperate with Project 8A.2, "Optical Phenomenology of High-Altitude Nuclear Detonations." In order to insure that there would be adequate coverage of the blast and shock phenomena, and to evaluate films of these events suitable for a future analysis from this standpoint. Films of all shots were examined, and in the course of the evaluation measurements were made of the two most promising, from a blast viewpoint—Shots Tight Rope and Blue Gill Triple Prime. These measurements were by no means as complete as those reported by Project 8A.2 (Reference 1) nor were they significantly different. The analysis of the results of these shots is to be carried out under another task for which the Laboratory has been funded.

Later, Project 1.2 was funded by Headquarters, Defense Atomic Support Agency, to carry out an investigation of the blast and shock effects of selected shots of the Dominic diagnostic series carried out at Christmas Island. The findings of these latter analyses are presented in this report. Analyses of the Fish Bowl events are to be reported under another task.

The author is indebted to Messers D. F. Hansen, M. P. Shuler, Jr., D. Barnes, and R. C. Schneiderhan of Edgerton, Germeshausen and Grier, Inc. for their cooperation.

The author acknowledges and is particularly indebted to C. F Dieter, A M Lyons, and C. L. Karmel for their contributions to this project.

CONTENTS

1. INTRODUCTION

The photography, which was carried out by Edgerton, Germeshausen, and Grier, Inc. (EG&G) for the U. S. Atomic Energy Commission and used for diagnostic purposes, was also usable for shock phenomena measurements. Shock position-time data could be derived from the films of various shots, and from such data peak shock overpressure as a function of distance can be calculated.

1.1 Objectives. The primary objectives were:

a. To augment the data available for the empirical free-air pressure distance curve (Reference 2), and to investigate the effect of increased yields and varying altitudes on scaling.

b. To obtain basic shock radius-time data in a non-homogeneous atmosphere in order to investigate the effects of a real atmosphere on air shocks resulting from shots fired in free air.

1.2 Background. The empirical free-air pressure distance curve for 1 kt at sea level conditions (Reference 2) was based upon nine free-air shots which ranged in yield from 1 kt to 540 kt and in altitude from approximately 3900 feet (MSL) to 10,000 feet (MSL). The air drops of Dominic presented an opportunity to extend the range of yields and altitudes of free-air bursts that might be applied to the standard curve

The investigation of the effect of the non-homogeneous atmosphere on shock propagation has been restricted to large surface bursts and to Shot Cherokee. The surface bursts were of limited value because of the apparent focusing of energy upward which could not be separated absolutely from the non-homogeneous effects (References 3 and 4). The Cherokee data (Reference 5) were also limited because of the large bombing error and the uncertainties of the canister positions. In a real atmosphere the shock velocity is greater in the upward direction (non-homogeneous) than it is horizontally at a given distance. This effect can best be detected on devices of large yield; it was hoped that these differences in the vertical (upward) and horizontal shock radii would be measureable on the large-yield Dominic shots

1.3 Shots. Ten shots covering a broad range of yields and altitudes were examined in detail. To meet the objectives and keep the analysis within reasonable bounds, four shots were selected. The primary basis of choice was yield, and, of course, what was measureable in the film. The four shots selected, together with other pertinent information, are presented in Table 1

TABLE 1 SHOT DATA

Code Name	Yield*	Height of Burst (HOB)	Air Pressure at HOB	Air Temperature at HOB
Rinconada	0.815±.025 MT	9,105 ft	733 mb	11.2° C
Bighorn	7.65±.30 MT	11,810 ft	663 mb	8.6° C
Housatonic	9.96±.06 MT	12,130 ft	656 mb	7.0° C
Sunset	0.810±.03 MT	5,000 ft	849 mb	16.0° C

* Total fireball yield (t^0 scaling)

2. ANALYTICAL METHODS

Radius-time data obtained from the films were fitted by the method of least squares, with a smooth empirical function which could be differentiated to give the shock velocity as a function of distance. There were two fitting functions used in this analysis.

2.1 Surface Fitting Functions. For the surface data in the Mach region and other non-free-air phenomena the function used was a polynomial (Reference 6) of the form:

$$\log r = C + C_1 (\log t) + C_2 (\log t)^2 + \ldots C_n (\log t)^n \qquad (1)$$

Differentiation yields:

$$U = \dot{r} = \frac{r}{t}\left[C_1 + 2C_2 \log t + \ldots nC_n (\log t)^{n-1}\right] \qquad (2)$$

where r = shock distance from surface zero

t = time

$C, C_1 \ldots C_n$ = constants

n = order of polynomial (usually between 2 and 6)

U = shock velocity

2.2 Free-Air Fitting Functions. For the free-air radius-time data the fitting function was of the form:

$$t = \frac{r}{A} - \frac{1}{A}\int_{r_0}^{r_f} \frac{B^{1.4}}{B^{1.4} + r^{1.4}}\, dr + C \qquad (3)$$

Differentiation yields:

$$U = \dot{r} = A\left[1 + \left(\frac{B}{r}\right)^{1.5}\right] \qquad (4)$$

where A, B, and C are constants

r = shock radius

t = time

U = shock velocity

The derivation of Equations 3 and 4 may be found in Reference 7.

2.3 Computation of Pressure. The shock velocity derived from both fitting methods was used to calculate overpressures by use of the relation:

$$\frac{U^2}{C_o^2} = \frac{\left[K_s\ (Q + 1) + 1\right]}{\gamma_o\left[(Q + 1)\ (K_s - 1) + 1 + K_o\right]} \qquad (5)$$

so that

$$P_s = \frac{P_o}{2K_s}\left[-B + \sqrt{B^2 - 4K_s\ \gamma_o\ M^2\ (K_o - K_s)}\right] \qquad (6)$$

where $B = 1 + K_s - \gamma_o M^2 (K_s - 1)$

$Q = P/P_o$

P = peak shock overpressure

$K_s = (\gamma_s + 1)/(\gamma_s - 1)$

$K_o = (\gamma_o + 1)/(\gamma_o - 1)$

γ_s = ratio of specific heats at shock front

γ_o = ratio of specific heats in front of shock

M = Mach number, U/C_o

C_o = ambient speed of sound

2.4 Scaling of Data. In order to compare the homogeneous free-air and surface data with previous work, the data were reduced to standard sea level conditions

P_{oo} = 14.7 psi

T_{oo} = 288°K

using Sachs scaling (Reference 8).

3. RESULTS AND DISCUSSIONS

The films used in the analysis are listed in Table 2.

TABLE 2 PHOTOGRAPHIC PLAN

Shot	EG & G Film No.	Photographic Station	Range to W.P. (ft)	Nominal Focal Length (mm)	Frame Rate (fr/sec)
Bighorn	111018	A/C 298	162,915	75	95
	111019	A/C 299	164,155	75	99
Housatonic	120262	A/C 299	196,570	50	76
Rinconada	109015	A/C 299	99,100	75	100
	109014	A/C 298	99,720	75	110
Sunset	114756	A/C 298	89,290	75	110

All of the data presented were derived from films taken from aircraft. Films obtained on the surface were not used, because the cloud cover obscured the growth of the free-air shock front after shock breakaway, and camera aiming angles were such that the surface was not observable.

The primary problems encountered in the films used were the uncertainty of aircraft position and the cloud cover which tended to obscure the surface phenomenology.

All in all the quality of the EG&G films was excellent, the Bighorn films were particularly good.

Usable free-air data were obtained for Bighorn, Housatonic, and Rinconada; surface radius-time data were measurable in the Bighorn and Sunset films.

3.1 Phenomenology. A series of photographs of Shot Bighorn is presented in Figures 1 through 5. The events illustrated by these photographs were observed—but were not necessarily measurable—on all of the shots examined.

Photograph 1 of the series was typical for all shots. The incident shock and the fireball are visible. Figure 2 shows the incident shock, and what appears to be a second shock* close behind. A clearly defined inner zone adjacent to the fireball, and apparently cooler than the fireball (i.e., the film is less dense), is also visible in this photograph. The cool inner zone appeared in all shots examined at about the time of shock breakaway. Figures 3 and 4 of the series, prints of the same frame, show the further development of the incident wave, the cooler inner zone, and the interaction of the shock and the surface. The incident shock is no longer visible in 5. but the interaction of the shock and the surface, and the Wilson cloud chamber effect are apparent. Note that the cool zone persists—it is visible on top of the rising fireball.

The inner zone radius-time data were reduced from the Bighorn, Mousetonic, and Rinconada films and were fitted by a function of the form of Equation 1 third order The results are shown in Figures 6, 7 and 8 respectively. Frontal velocity-distance data, Table 2, show that the front of the inner zone does not behave as a shock.

---

* The position time history of this apparent shock was not measurable

TABLE 3 INNER ZONE FRONTAL VELOCITY-DISTANCE DATA

Radius (ft)	Bighorn Velocity (ft/sec)	Rousatomic Velocity (ft/sec)	Rinconada Velocity (ft/sec)
2400	-	-	1500
2600	-	-	1140
2800	-	-	810
3200	-	-	220
4750	1970	-	
5000	1740	-	
5500	1310	-	
6000	910	1330	
6900	520	950	
7000	220	630	
8000	-	140	

No further investigation of this phenomenon was made.

3.2 Free Air Data. For Shots Bighorn, Rousatomic, and Rinconada the free-air shock arrival-time data were measured at burst height, parallel to the surface, i.e., in a homogeneous atmosphere; and vertically above weapon zero, i.e., in a non-homogeneous atmosphere. Plots of the basic radius-time data, both horizontal and vertical, together with the fitted curves and the coefficients of the fitting functions (Equation 2) are presented in the Appendix.

The horizontal and vertical shock arrival-time curves for Bighorn, Housatonic, and Rinconada are compared in Figures 6, 7, and 8. Although these curves indicate that the shock was growing faster vertically than horizontally, the scatter of the radius-time data, particularly the vertical data, was great enough to cast serious doubt on the validity of differences in velocities. Refer to Figures A.1 through A.6 in the Appendix. Further, there is another problem, and that is the fitting function itself. The function used, Equation 3, was designed for use with the homogeneous free-air situation and not for the vertical free-air case. The effects of this function upon vertical radius-time data will require further investigation.

Conclusions pertaining to shock propagation in a non-homogeneous atmosphere based upon these data are not warranted at this time.

Peak shock overpressure-distance data in the homogeneous atmosphere for Bighorn, Housatonic, and Rinconada may be seen in Figures 9, 10 and 11.

3.5 Scaled Free-Air Data. The homogeneous free-air shock arrival-time data for Bighorn, Housatonic, and Rinconada reduced to 1 kt at sea level conditions are presented in Figure 12. All three sets of data are in agreement with the standard curve.

The reduced peak shock overpressure-distance data are compared to the empirical 1 kt free-air curve in Figure 13. Bighorn and Housatonic are in close agreement with the curve. The slope of the Rinconada data is slightly different but lies within the scatter of the standard curve.

Based solely on the strength of the agreement of these radius-time and overpressure-distance data it appears as though the empirical free-air curves are valid for yields as high as ~ 10 Mt and heights of burst as high as 12,000 feet.

3.4 Surface Data. The interaction of the shock front and the ocean surface appeared as an ellipse in the aircraft films of several shots. Measurements made along the major axis of the ellipse could be read as a diameter provided that the major axis coincided with the line formed by the plane of measurement and the surface plane.

It was possible to make useful surface measurements on Bighorn and Sunset. The surface radius-time data are compared to curves derived from the near-ideal arrival time height of burst (HOB) charts of Reference 9, in Figure 14.

The Sunset experimental radius-time data and the scaled HOB arrival time data are in surprisingly good agreement.

The Bighorn experimental data are displaced from the scaled HOB chart radius-time curve, but these data lie within the stated reliability limits (± 10%) of the HOB chart (Reference 9). The divergence of the Bighorn data from the curve increases with time; this increase is attributed to the decrease in the optical magnification caused by the aircraft moving farther away from weapon zero.

Peak shock overpressure-distance data were calculated in the Mach region. (The Mach stem was not visible; it was assumed to have been formed by the time the surface shock had reached a distance equal to the height of burst.) These experimental data are compared

to surface pressure-distance curves derived from the near-ideal over-pressure height of burst charts (Reference 9) in Figures 15 and 16.

The fragment of the Sunset pressure-distance data is not in agreement with the near-ideal curve in the comparable regions. (If the experimental Sunset data were extrapolated — a dangerous procedure — the extrapolated data would appear to agree with the near-ideal curve.)

The Bighorn pressure distance data show a faster decay than the near-ideal curve, but the differences in pressures at corresponding distances are relatively small; the maximum is no more than 15%. The stipulated reliability attached to the near-ideal peak shock overpressure HOB chart is ± 15% (Reference 9).

Superficially, it would appear that the near-ideal height of burst charts could be used within the reliability limits stipulated by Reference 9 up to yields of ~ 8 Mt.

4. CONCLUSIONS AND RECOMMENDATIONS

Based solely upon the agreement of the scaled radius-time and peak shock overpressure-distance data of Shots Bighorn, Housatonic, and Rinconada with the standard free-air curves, it appears as though the empirical free-air curves are valid for use with yields up to ~ 10 Mt and to heights of bursts up to ~ 12,000 feet.

Based upon surface radius-time data of Bighorn and Sunset, and pressure-distance data in the Mach region obtained from Bighorn it appears — at least superficially — as though the near-ideal height of burst curves can be used within the reliability limits stipulated in Reference 9 up to yields of ~ 8 Mt.

Although the horizontal and vertical radius-time data obtained in free air indicated that the vertical shock growth was faster than that of the horizontal, the scatter of the data was great enough to make the apparent differences in the velocities very doubtful. Conclusions are not warranted.

The scatter of these radius-time data would have been decreased considerably, perhaps by an order of magnitude, if the smoke rocket technique could have been used; (e.g., the Redwing-Cherokee experiment, Reference 4). If such experiments as those of the Dominic series were ever carried out again, the use of smoke rockets is recommended.

Figure 1 Shot Bigbee, Station 200, 0.19 second. (Film 111018, EG&G Photo)

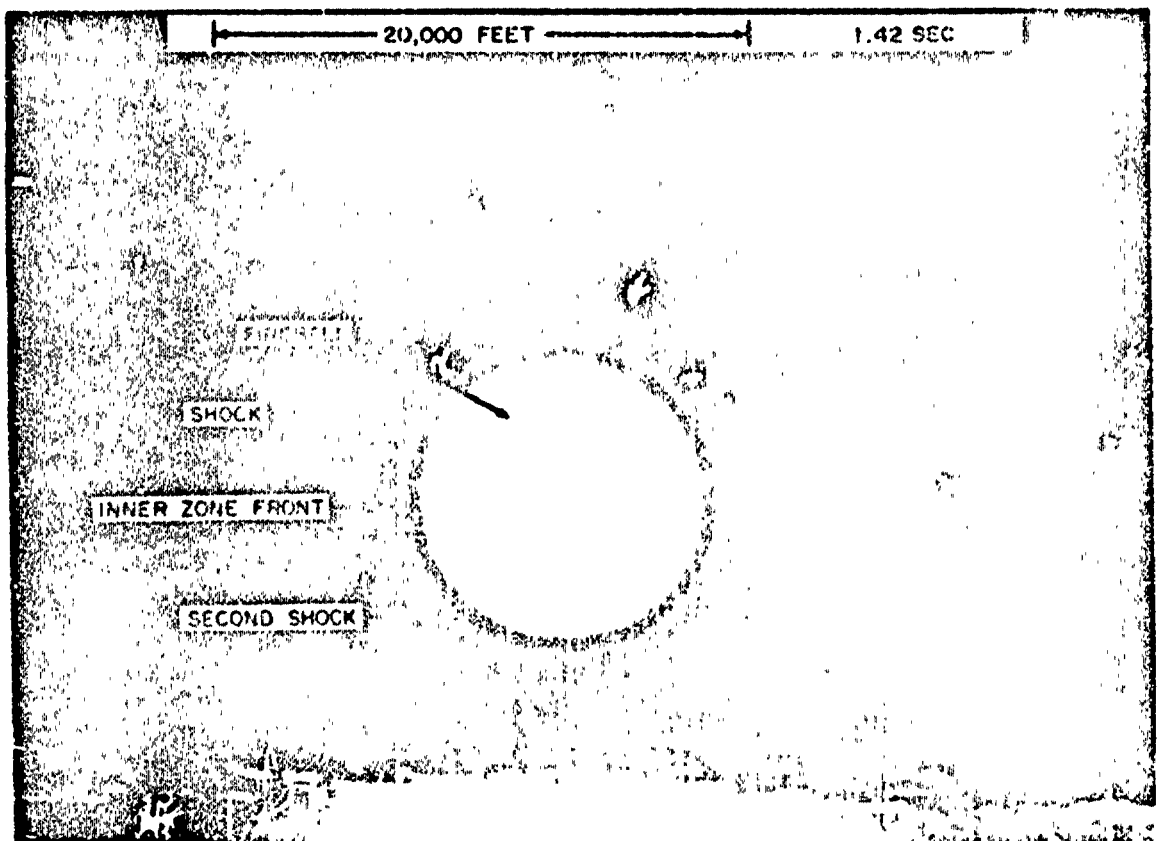

Figure 2 Shot Tiger, Station 298, 1.42 seconds. (Film 111013, EG&G Photo)

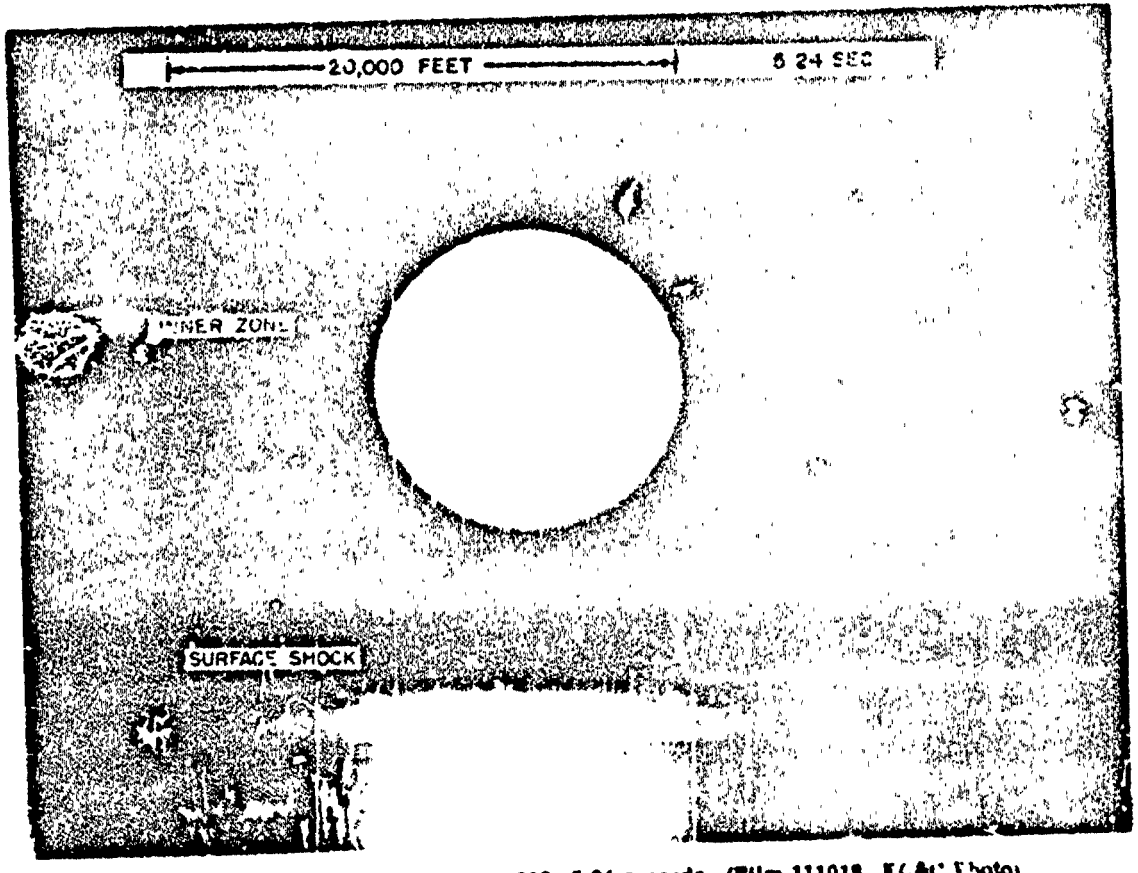

Figure 3 Shot Bigger, Station 298, 5.24 seconds. (Film 111018, EG&G Photo)

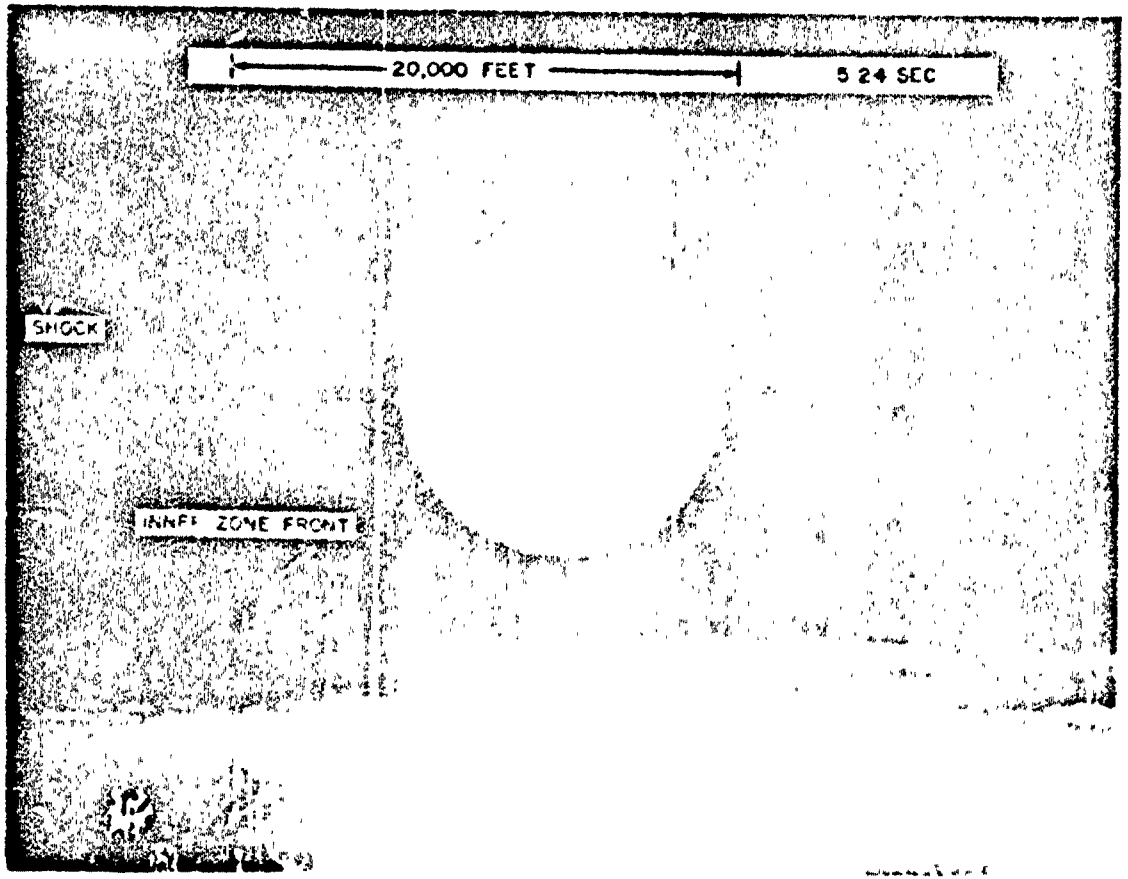

Figure 4 Shot Typhoon, Station 298, 5.24 seconds. (Film 111018, EG&G Photo)

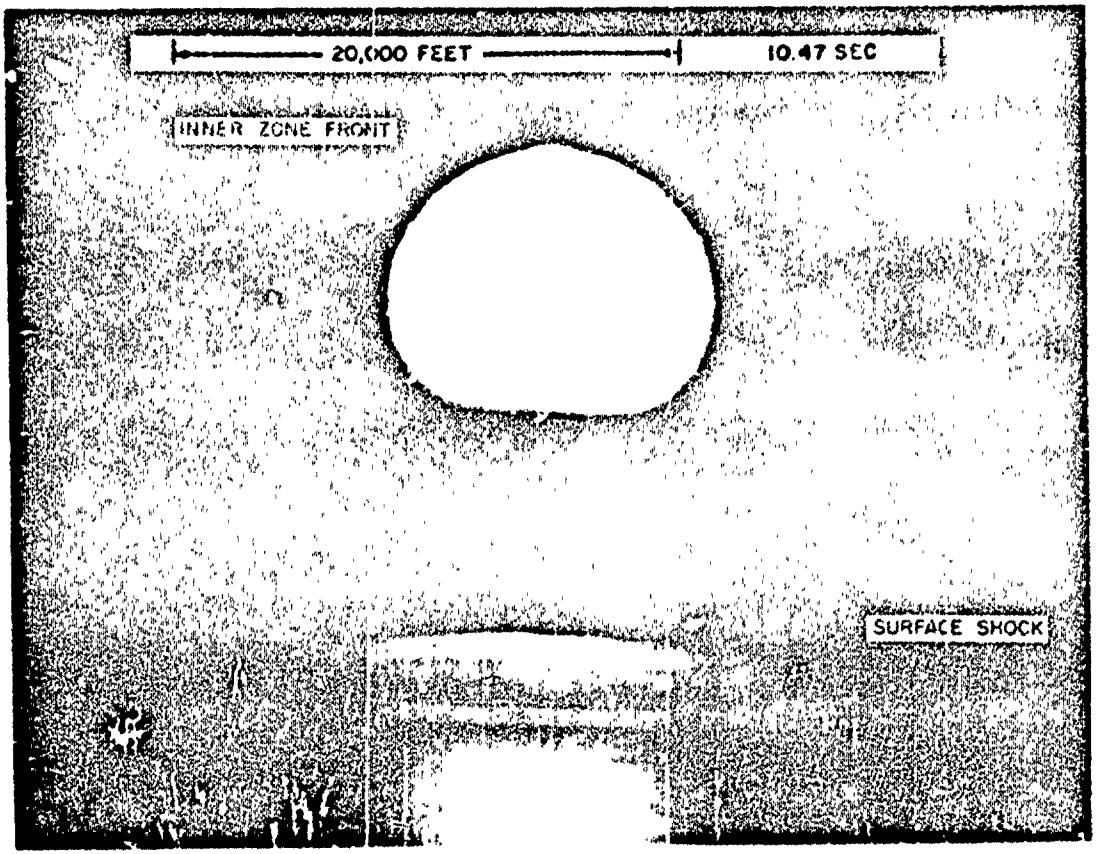

Figure 5 Shot Bighorn, Station 298, 10.47 seconds. (Film 111018, Fi&Pi Photo)

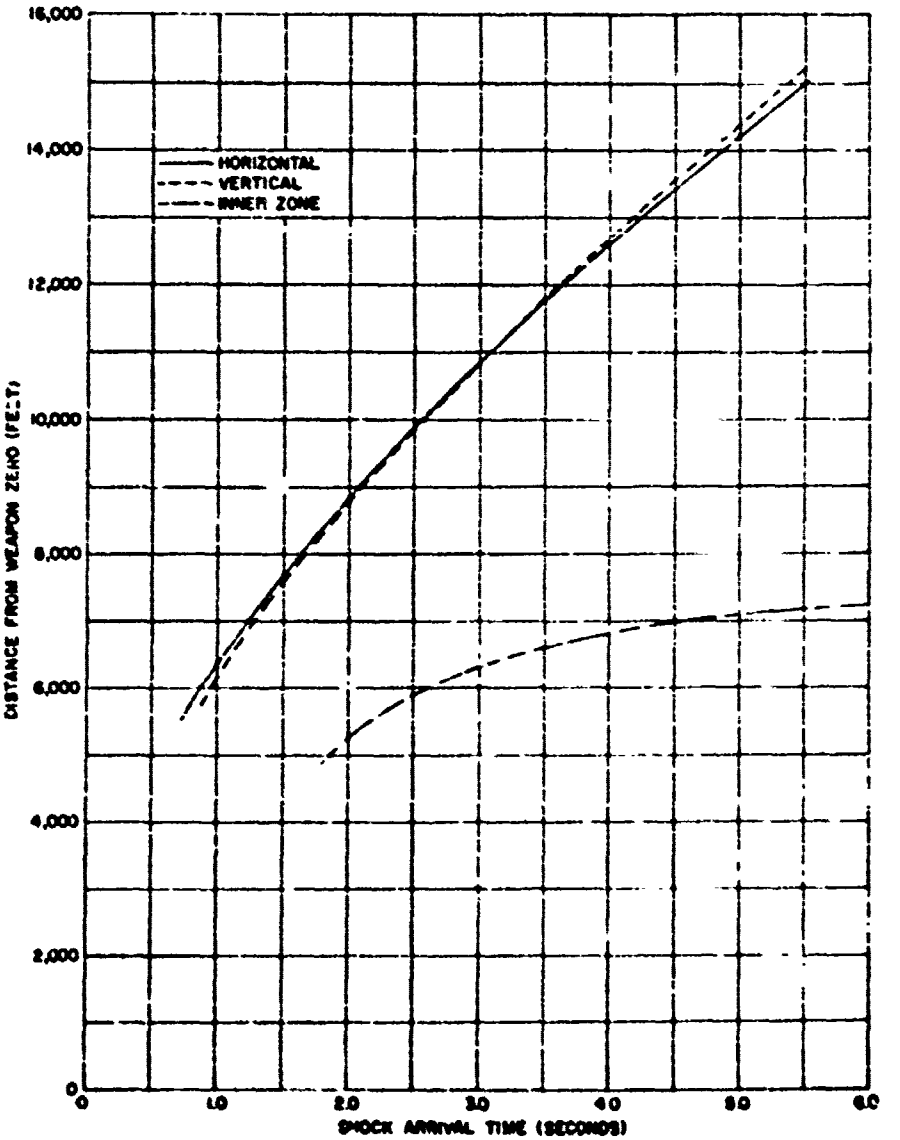

Figure 6 Free-air, shock-arrival time and inner zone data, Shot Bighorn

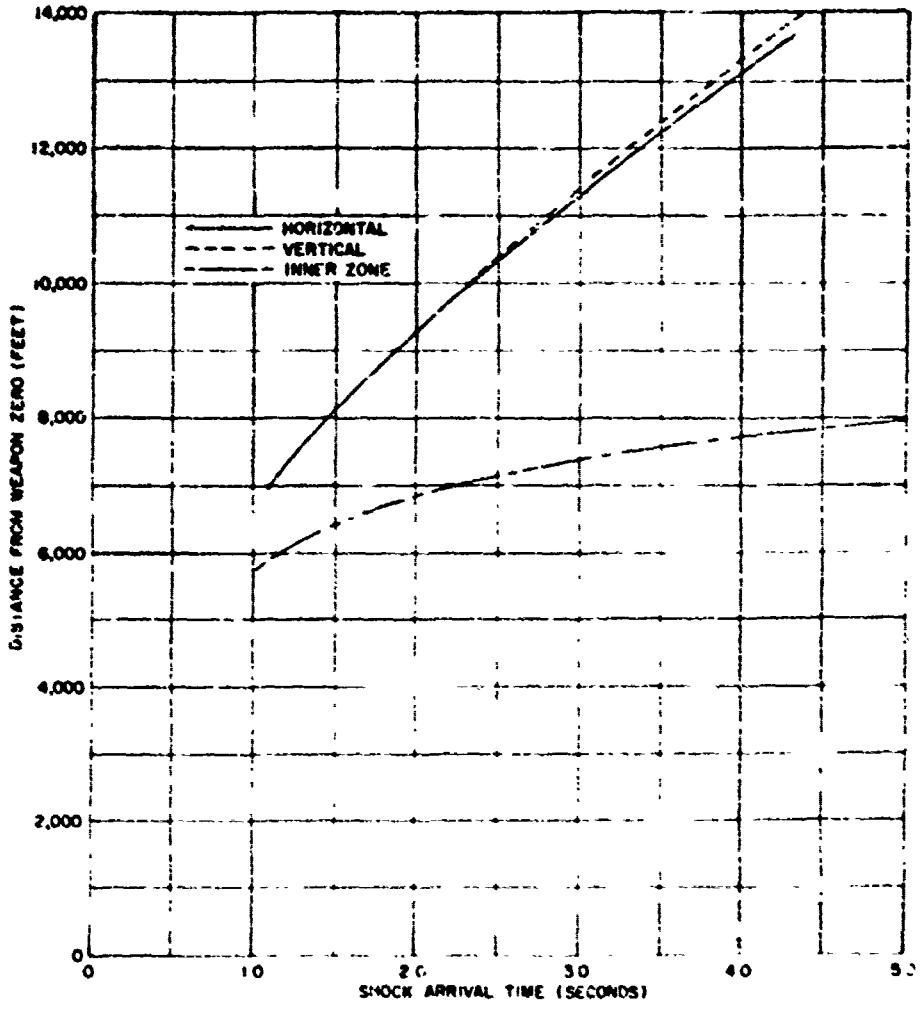

Figure 1 Free-air shock-arrival time and inner zone data, Red Devastator

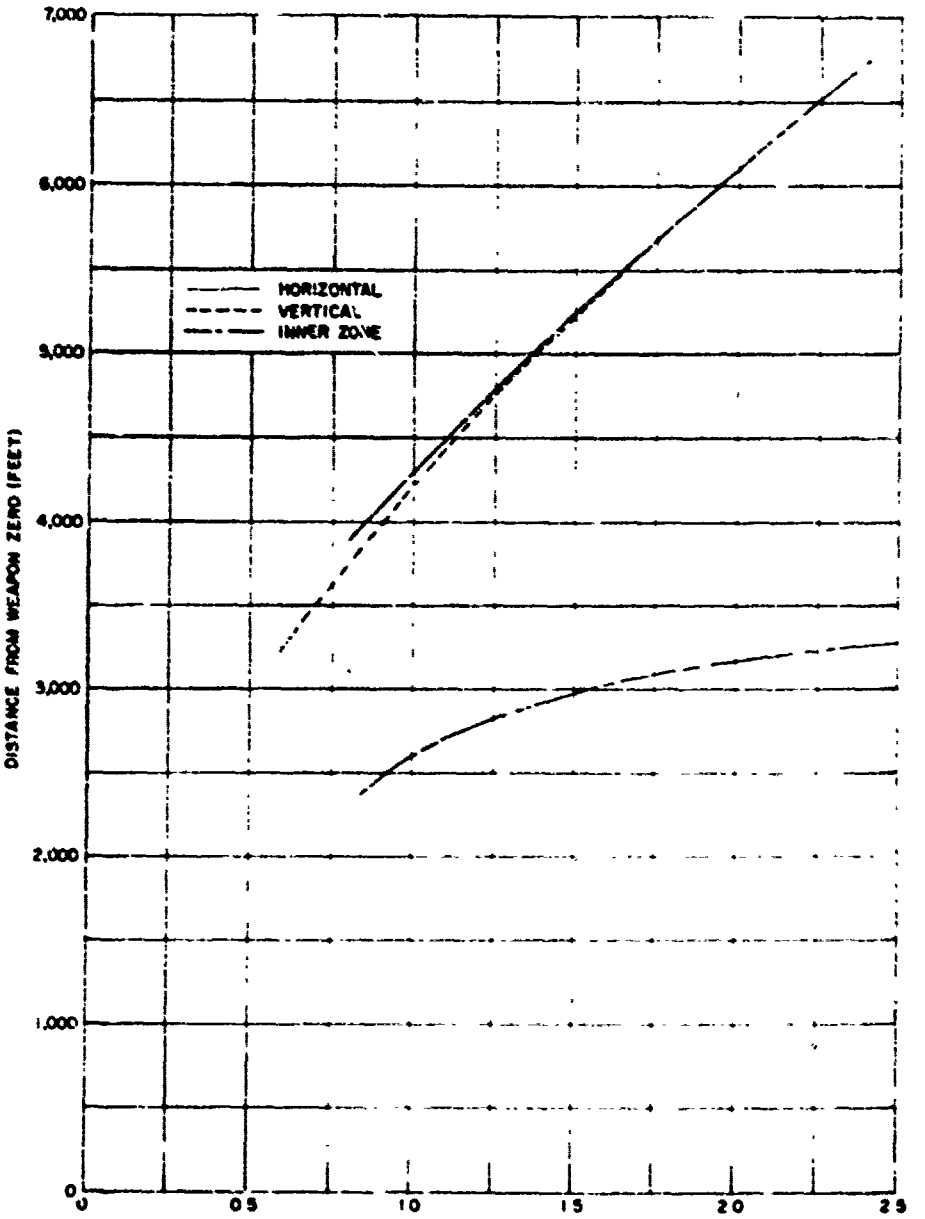

Figure 8 Free-air, shock-arrival time and inner zone data, Shot Rinconada

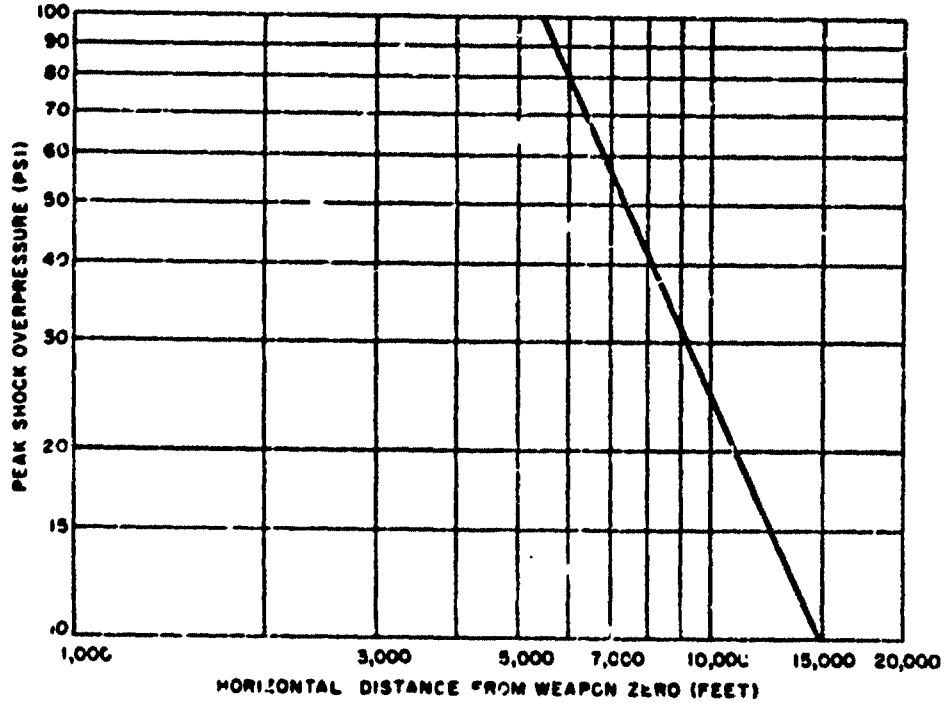

Figure 9 Free-air, peak-shock overpressure versus horizontal distance from weapon zero, Shot Bighorn.

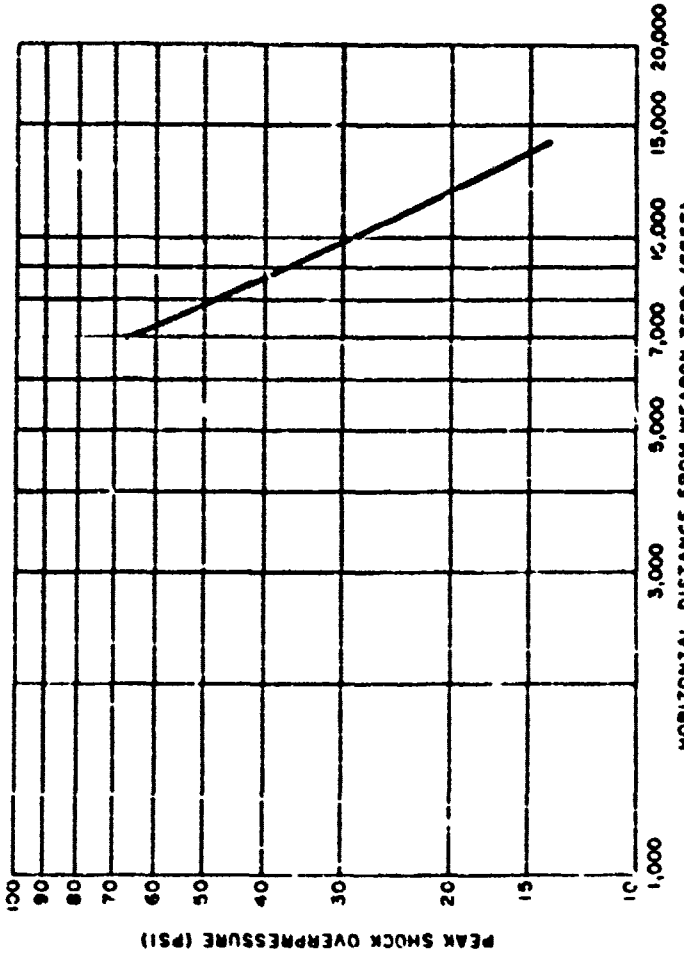

Figure 10 Free-air peak-shock overpressure versus horizontal distance from weapon zero, Shot Housatonic.

SECRET

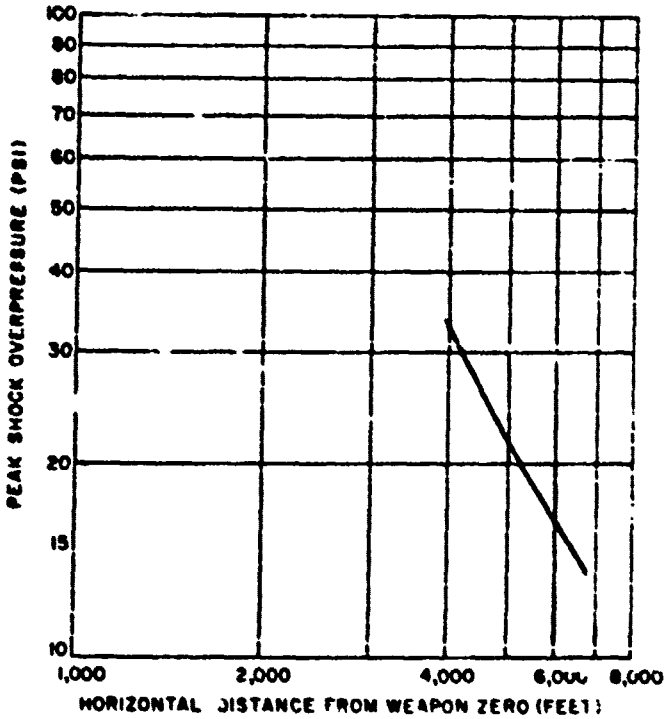

Figure 11 Free-air, peak-shock overpressure versus horizontal distance from weapon zero, Shot Rinconada

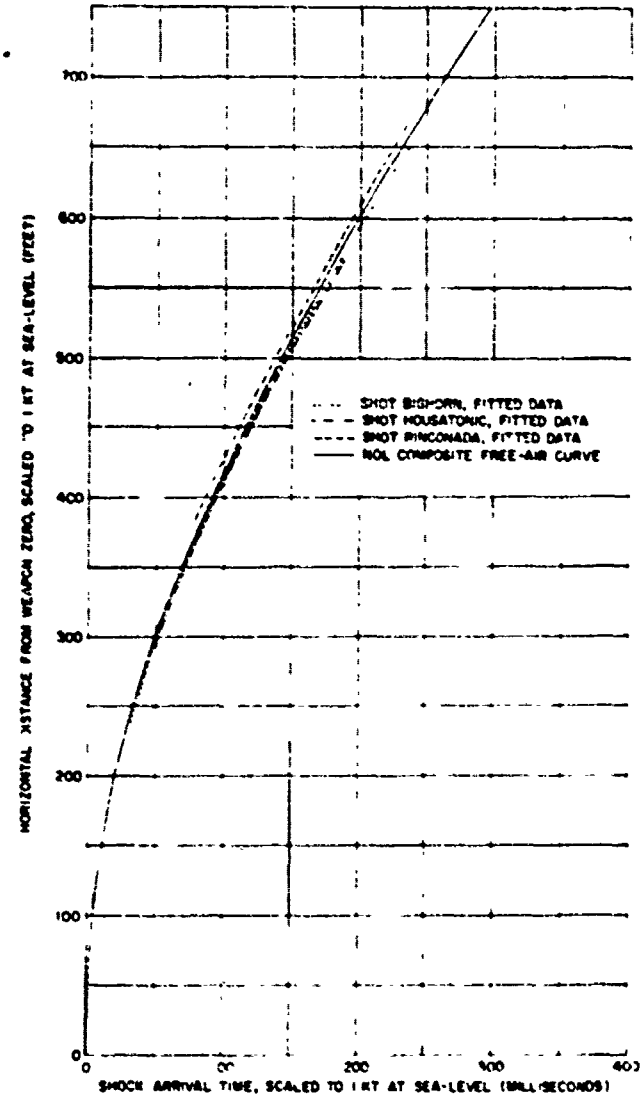

Figure 18 Free air shock arrival time data for Shots Bighorn, Housatonic and Pinconada

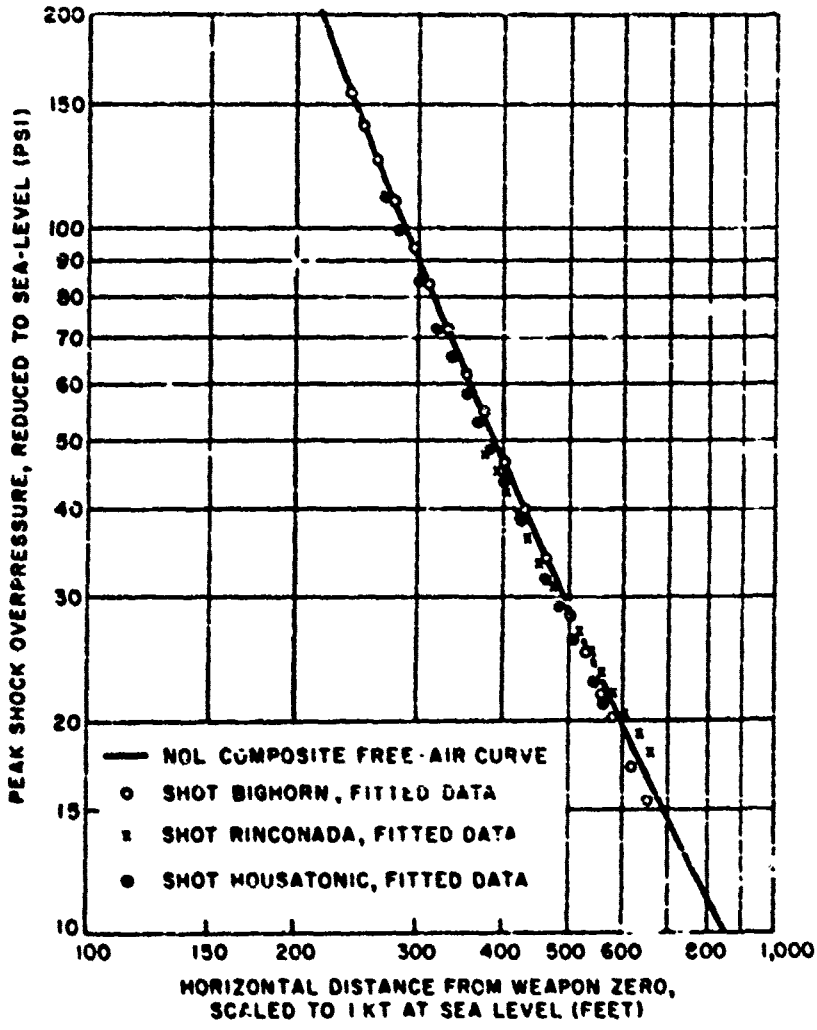

Figure 13 Free-air pressure-distance data for Shots Bighorn, Housatonic, and Rinconada, scaled to 1 kt at standard sea level conditions.

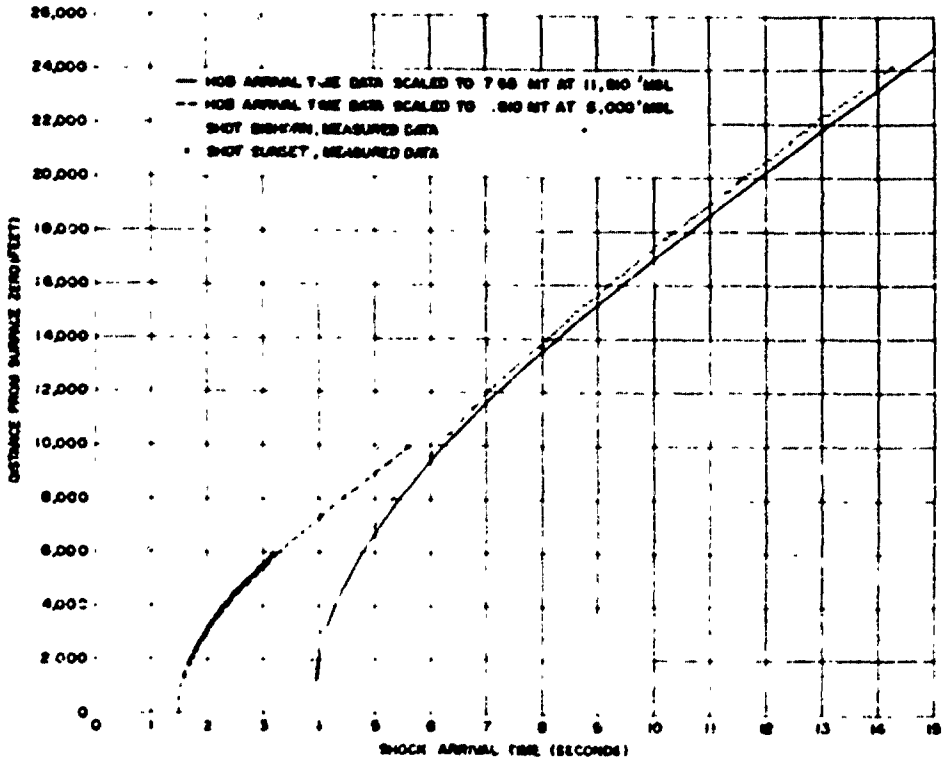

Figure 10. Preliminary [illegible] arrival time data for Shots Bighorn and Sunset, compared to data scaled from [illegible] curve ROE Chart.

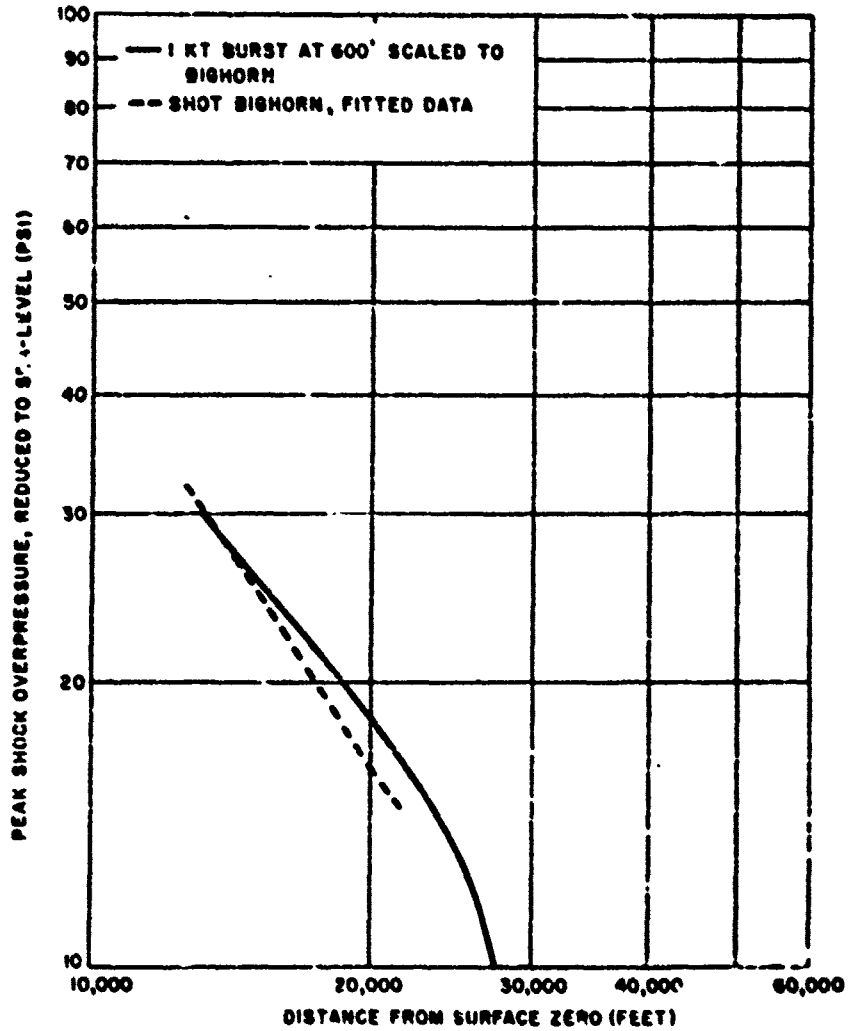

Figure 15 Surface, pressure-distance data in the Mach region for Shot Bighorn, compared to data scaled from near-ideal overpressure HOB charts.

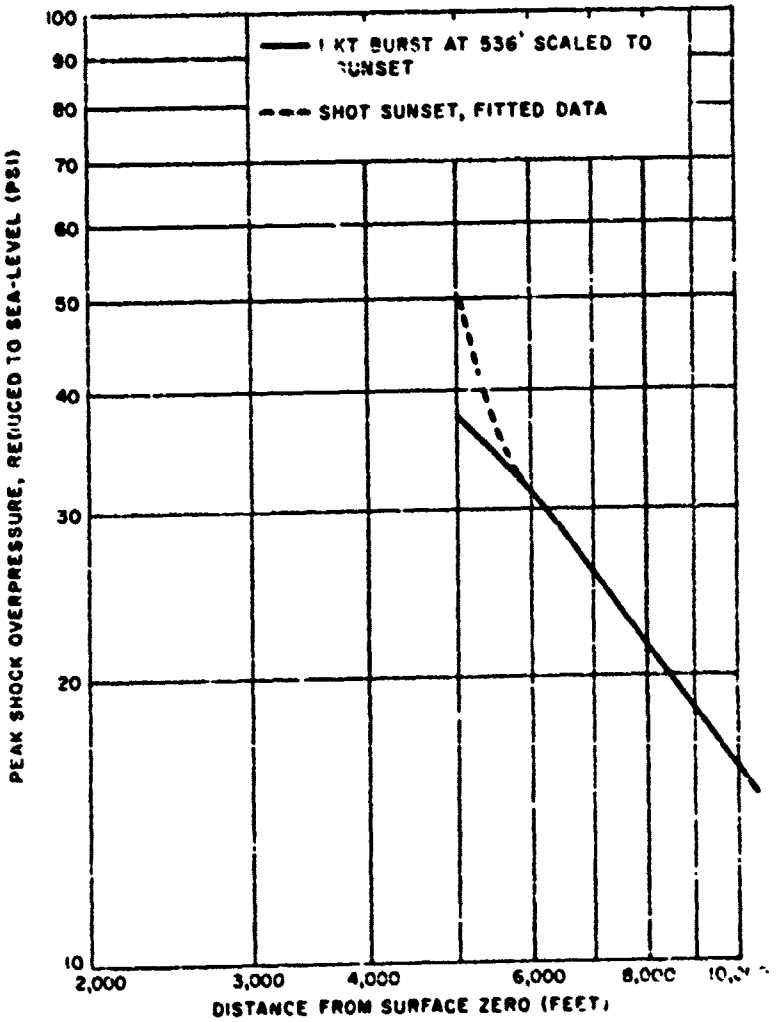

Figure 16 Surface, pressure–distance data in the Mach region for Shot Sunset, compared to data scaled from near-ideal overpressure HOB charts.

APPENDIX

BASIC RADIUS-TIME DATA

The basic radius-time data are given in Figures A.1 through A.6. The coefficients for Equation 3 used to fit the free-air data of Shots Bighorn, Bonnatonic, and Rinconada are given in Table A.1.

TABLE A.1 COEFFICIENTS FOR EQUATION 3

Shot	A	B	C
Bighorn			
Horizontal	952.04	10473.15	0.033396
Vertical	1174.56	7991.33	-0.069573
Bonnatonic			
Horizontal	963.15	11167.38	-0.016609
Vertical	1271.33	7887.87	-0.155644
Rinconada			
Horizontal	1169.47	3492.83	-0.185550
Vertical	944.78	5183.97	0.084946

The coefficients for Equation 1 (third order) which were used to fit the surface data of Shots Bighorn and Sunset are given in Table A.2.

TABLE A.2 COEFFICIENTS FOR EQUATION 1 (THIRD ORDER)

Shot	C	C_1	C_2	C_3
Bighorn	-51.29	45.50	-10.70	0.8566
Sunset	-585.52	901.35	-142.47	13.52

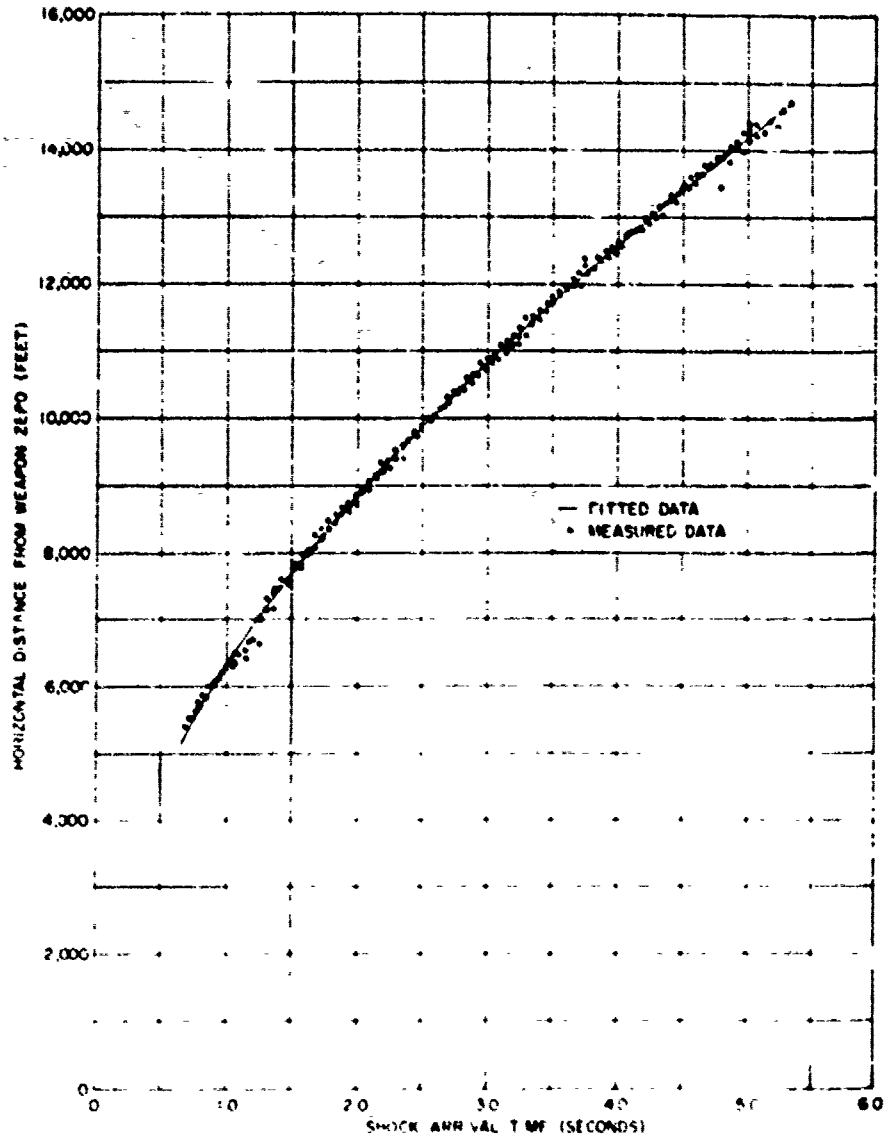

Figure A-1. Horizontal, free air shock-off velocity. Shot Hightop

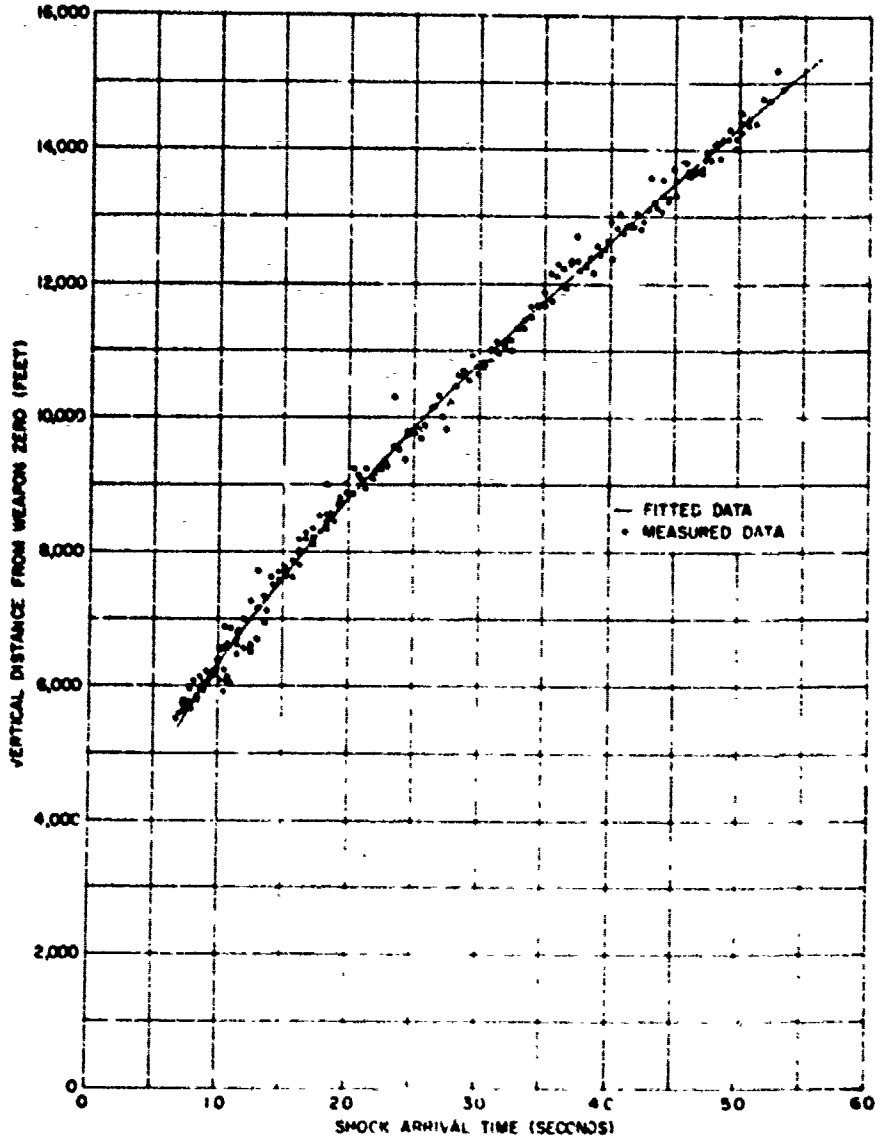

Figure A 2 Vertical, free-air, shock-arrival time, Shot Bighorn

SECRET

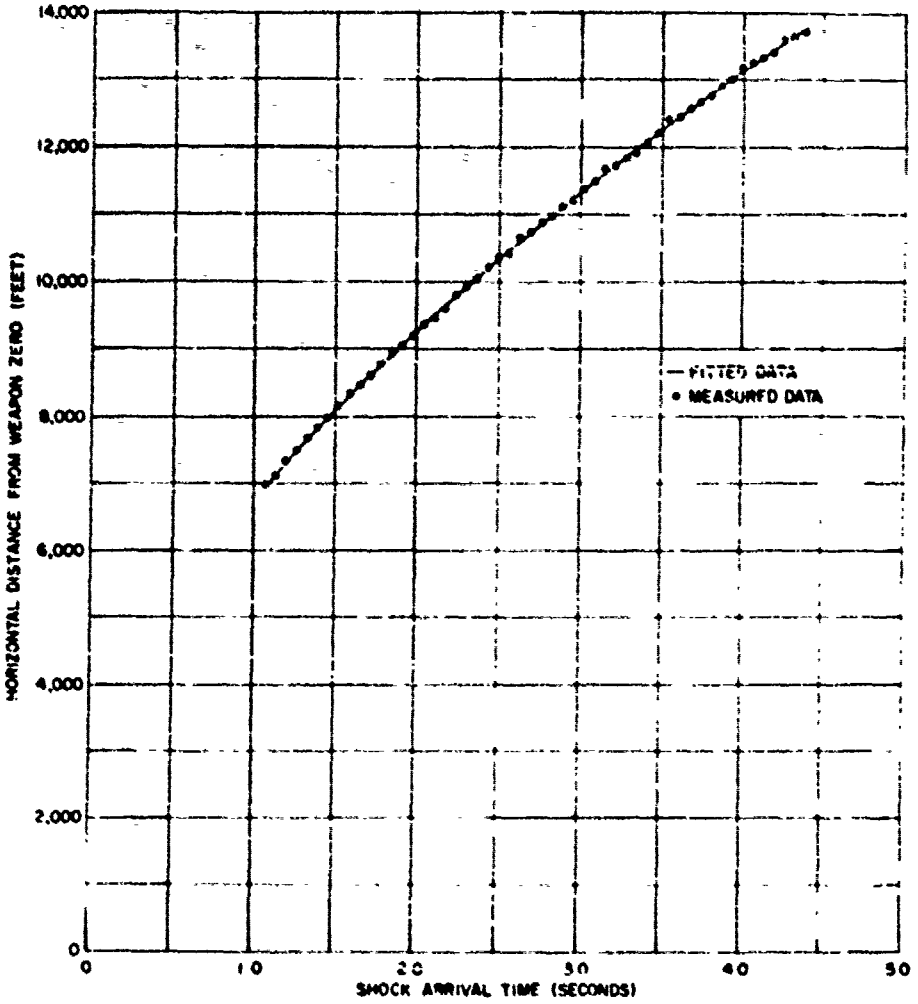

Figure A 3 Horizontal, free-air, shock-arrival time Short Nuclear

[redacted]

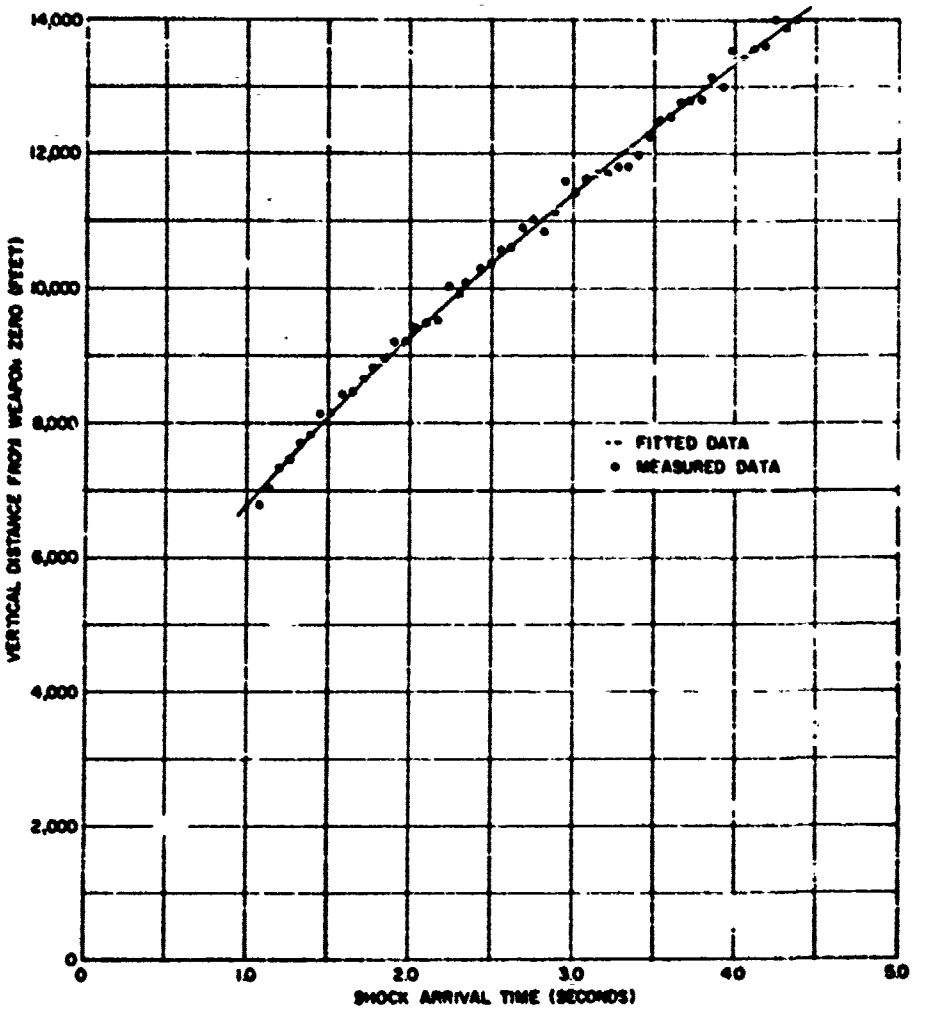

Figure 4.4 Vertical free-air, shock-arrival time, Shot Hoosickwic.

[redacted]

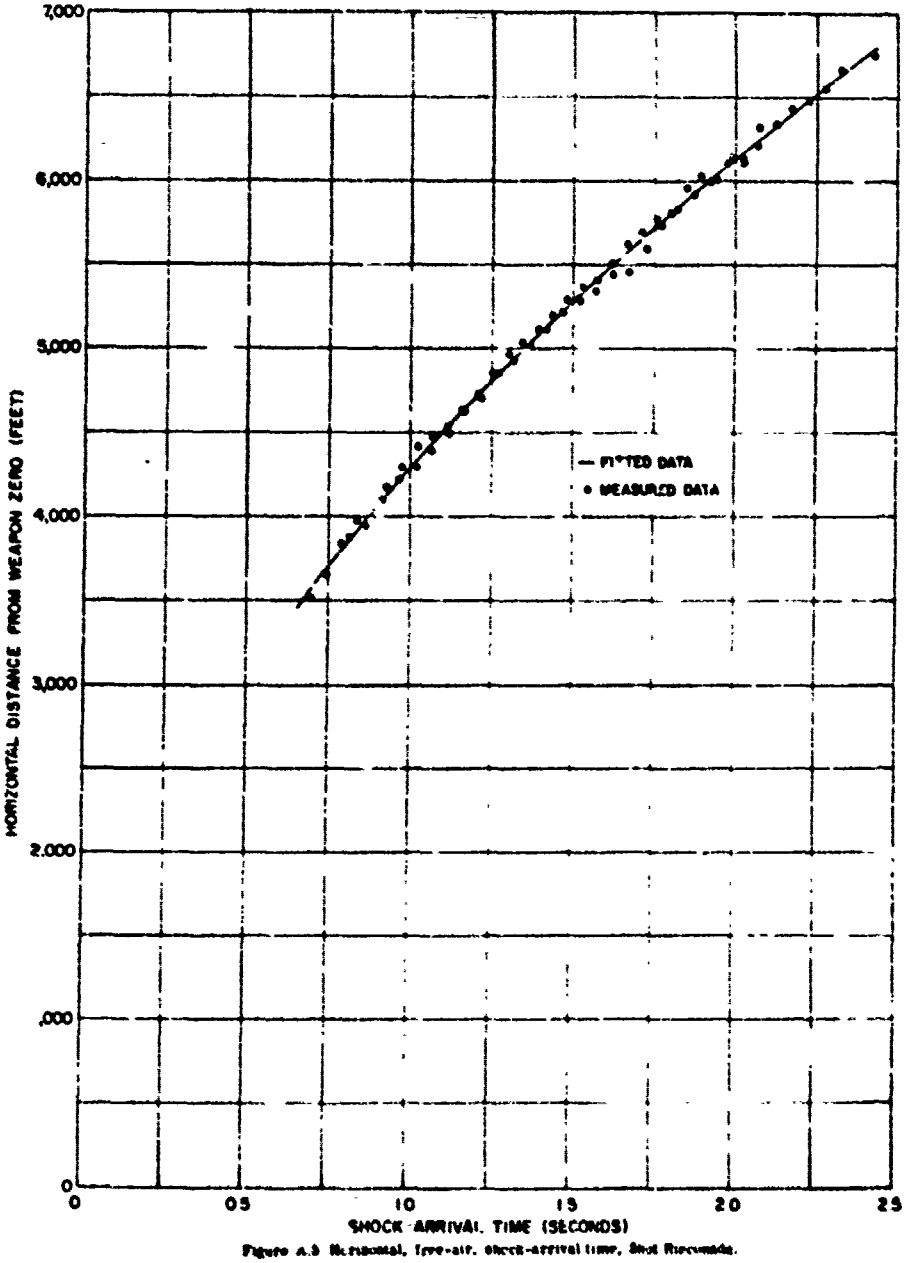

Figure A.3 Horizontal, free-air, shock-arrival time, Shot Riccomide.

[redacted]

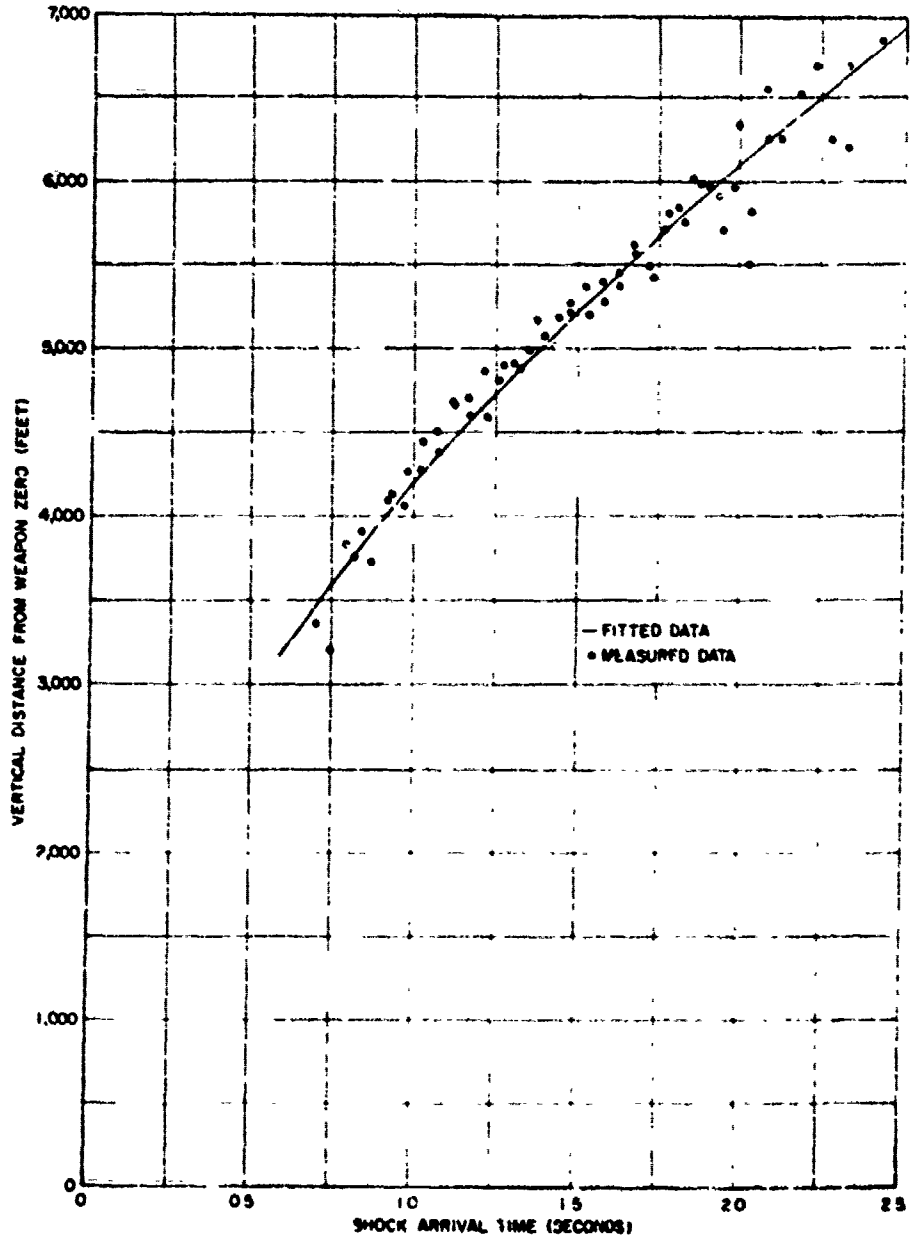

Figure A 6 Vertical, free-air, shock-arrival time, Shot Bluegill

[redacted]

REFERENCES

1. D. F. Hasser and others; "Selected Excerpts From Defense Atomic Support Agency Project 8A.2 Project Officers Report Fish Bowl Series (U)," EG and G Report No. E2650, Contract No. DA 49-146-XZ 135; Edgerton, Germeshausen, and Grier, Inc., Boston, Mass; 30 August 1963; Secret Restricted Data.

2. J. F. Moulton, Jr.; "Nuclear Weapons Blast Phenomena; DASA 1200, Vol. I, March 1960; Defense Atomic Support Agency, Washington 25, D. C.; Secret Restricted Data.

3. P. Mahlon and others; "Blast Pressures and Shock Phenomena Measurements by Photography," Projects 1.1a, 1.1b, and 1.1d, Operation CASTLE, WT 902; September 1955; U. S. Naval Ordnance Laboratory, White Oak, Maryland; Secret Restricted Data.

4. L. J. Sullivan and P. Mahlon; "Airblast and Shock Phenomena by Photography," Operation REDWING, Project 1.3, WT 1303; September 1959; U. S. Naval Ordnance Laboratory, White Oak, Maryland; Secret Formerly Restricted Data.

5. R. A. Randall and J. A. Fava, "Measurement of Free-Air Atomic-Blast Pressures," Project 1.4, Operation REDWING, WT 1304, February 1959; Air Force Cambridge Research Center, Bedford, Mass.; Secret Formerly Restricted Data

6. D. L. Lakto and L. J. Sullivan; "The Treatment of Airblast Radius-Time and Pressure Distance Data by the Use of Polynomial Approximations with Application to Pentolite Data," NOLTR 62-85, U. S. Naval Ordnance Laboratory, White Oak, Maryland; Unclassified.

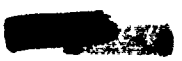

7. J. F. Moulton and P. Hunlon; "Peak Overpressure Vs. Distance in Free Air," Project 6.13, Operation IVY, WT 613; March 1953; Naval Ordnance Laboratory, White Oak, Maryland; Secret Restricted Data.

8. R. G. Sachs; "The Dependence of Blast on Ambient Pressure and Temperature;" Ballistic Research Laboratories Report No. 466; Aberdeen Proving Ground, Maryland; 15 May 1944; Unclassified

9. J. F. Moulton, Jr.; "Nuclear Weapons Blast Phenomena," DASA 1200, Vol. II; March 1960; Defense Atomic Support Agency, Washington 25, D. C.; Secret Formerly Restricted Data.

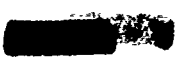

[redacted]

[redacted]

Address Distribution Category 12

ARMY ACTIVITIES

1 CHIEF OF R & D DA
2 AC OF S INTELLIGENCE DA
3 CHIEF OF ENGINEERS DA
4- 5 ARMY MATERIAL COMMAND
6- 7 U S ARMY COMBAT DEVELOPMENTS COMMAND
8 U S ARMY CDC NUCLEAR GROUP
9 U S ARMY ARTILLERY BOARD
10 U S ARMY AIR DEFENSE BOARD
11 U S ARMY COMMAND AND GENERAL STAFF COLLEGE
12 U S ARMY AIR DEFENSE SCHOOL
13 U S ARMY CDC ARMOR AGENCY
14 U S ARMY CDC ARTILLERY AGENCY
15 U S ARMY CDC INFANTRY AGENCY
16 U S ARMY ORDNANCE & GUIDED MISSILE SCHOOL
17 U S ARMY CDC CBR AGENCY
18 ENGINEER SCHOOL
19 ARMED FORCES INSTITUTE OF PATH
20 ARMY MEDICAL RESEARCH LAB
21 WALTER REED ARMY INST OF RES
22 ENGINEER RESEARCH & DEV LAB
23 WATERWAYS EXPERIMENT STATION
24 PICA[illegible] ARSENAL
25 DI[illegible] ORDNANCE FUZE LABORATORY
26- 27 BALLISTIC RESEARCH LABORATORY
28 FRANKFORD ARSENAL
29 WATERVLIET ARSENAL
30- 31 WHITE SANDS MISSILE RANGE
32 U S ARMY MOBILITY COMMAND
33 U S ARMY WEAPONS COMMAND
34 U S ARMY MUNITIONS COMMAND
35 U S ARMY ELECTRONIC PROVING GROUND
36- 37 U S ARMY CDC COMBAT SERVICE SUPPORT GROUP
38 THE RESEARCH & ANALYSIS CORP
39 WHITE SANDS SIGNAL SUPPORT AGENCY
40 U S ARMY NUCLEAR DEFENSE LABORATORY
41 U S ARMY CDC AIR DEFENSE AGENCY
42 U S ARMY COLD REGION RES & ENG LABORATORY
43 U S ARMY CORPS OF ENG NUCLEAR CRATERING
44 UNITED STATES CONTINENTAL ARMY COMMAND
45 U S ARMY CDC COMBINED ARMS GROUP
46- 47 HQ ARMY MATERIAL COMMAND,SANDIA
48 US ARMY ENGR,REDSTONE & ENGR,LABS

NAVY ACTIVITIES

49- 50 CHIEF OF NAVAL OPERATIONS OP03EG
51 CHIEF OF NAVAL OPERATIONS OP-76
52 CHIEF OF NAVAL OPERATIONS OP-96
53- 54 CHIEF OF NAVAL OPERATIONS CODE 811
55- 57 CHIEF BUREAU OF NAVAL WEAPONS DLI-3
58- 62 CHIEF BUREAU OF NAVAL WEAPONS RRAC-221
63 CHIEF BUREAU OF SHIPS CODE 423
64 CHIEF BUREAU OF YARDS & DOCKS CODE 74
65 DIR, NAVAL RESEARCH LABS
66- 67 U S NAVAL ORDNANCE LABORATORY
68 MATERIAL LABORATORY CODE 900
69 NAVY ELECTRONICS LABORATORY
70- 71 U S NAVAL BIOLOGICAL DEFENSE LAB
72 U S NAVAL CIVIL ENGINEERING LABORATORY
73 U S NAVAL SCHOOLS COMMAND U S NAVAL STATION
74 U S NAVAL POSTGRADUATE SCHOOL
75 U S FLEET SONAR SCHOOL U S NAVAL BASE
76 U S FLEET ANTI-SUBMARINE WARFARE SCHOOL
77 U S NAVAL SCHOOL CEC OFFICERS
78 U S NAVAL DAMAGE CONTROL TNG CENTER ABC
79 AIR DEVELOPMENT SQUADRON 5 VX-5
80 NAVAL AIR MATERIAL CENTER
81 U S NAVAL AIR DEVELOPMENT CENTER
82 U S NAVAL WEAPONS EVALUATION FACILITY
83 U S NAVAL MEDICAL RESEARCH INSTITUTE
84- 85 DAVID W TAYLOR MODEL
86 U S NAVAL ENGINEERING EXPERIMENT STATION
87 NORFOLK NAVAL SHIPYARD
88- 91 U S MARINE CORPS CODE 403M

AIR FORCE ACTIVITIES

92- 95 HQ USAF AFTAC-TD
96 HQ USAF AFMIC
97 HQ USAF AFSWP
98 HQ USAF AFCIN
97-101 HQ USAF AFCIN-401
102 AC OF S INTELLIGENCE HQ USAFE
103 RESEARCH & TECHNOLOGY DIV BOLLING AFB
104 BALLISTIC SYSTEMS DIVISION
105 HQ USAF AFNSPAA
106 TACTICAL AIR COMMAND
107 AIR DEFENSE COMMAND
108 AIR FORCE SYSTEMS COMMAND
109 RADC-RALD,GRIFFISS AFB
110 PACIFIC AIR FORCES
111 SECOND AIR FORCE
112-113 AF CAMBRIDGE RESEARCH CENTER
114-118 AFWL WLL-9 KIRTLAND AFB
119-120 AIR UNIVERSITY LIBRARY
121 SCHOOL OF AVIATION MEDICINE
122-124 AERONAUTICAL SYSTEMS DIVISION
125-126 USAF PROJECT RAND
127 AIR TECHNICAL INTELLIGENCE CENTER
128 HQ USAF AFOMO
129 HQ USAF AFXPDC

OTHER DEPARTMENT OF DEFENSE ACTIVITIES

130 DIRECTOR OF DEFENSE RESEARCH & ENGINEERING
131 ASST TO THE SECRETARY OF DEFENSE ATOMIC ENERGY
132 ADVANCE RESEARCH PROJECT AGENCY
133 WEAPONS SYSTEM EVALUATION GROUP
134 ASST SECRETARY OF DEFENSE INSTALLATION & LOGISTICS
135-138 DEFENSE ATOMIC SUPPORT AGENCY
139 FIELD COMMAND DASA
140 FIELD COMMAND DASA PCTA
141-142 FIELD COMMAND DASA FCW
143-144 DEFENSE INTELLIGENCE AGENCY
145 ARMED SERVICES EXPLOSIVES SAFETY BOARD
146 JOINT TASK FORCE-8
147 COMMANDER-IN-CHIEF PACIFIC
148 COMMANDER-IN-CHIEF ATLANTIC FLEET
149 STRATEGIC AIR COMMAND
150 CINCONAD
151-153 ASST SECRETARY OF DEFENSE CIVIL DEFENSE
154 DIR,DEFENSE INTELLIGENCE AGENCY
155-176 DEFENSE DOCUMENTATION CENTER

PCG CIVILIAN DISTR CAT. 6 1

175 AEROSPACE CORPORATION ATTN DOCUMENT
176 STANFORD RESEARCH INSTITUTE ATTN LIBRARY
177 RAMAN AIRCRAFT CORP ATTN DR. [illegible]LTON
178 UNITED RESEARCH SERVICES INC ATTN KAPLAN
179 FORD MOTOR CO ATTN HARDER
180 GENERAL ELECTRIC CO DEPT,ELEC,DIR

ATOMIC ENERGY COMMISSION ACTIVITIES

181-183 AEC WASHINGTON TECH LIBRARY
184-185 LOS ALAMOS SCIENTIFIC LAB
186-190 SANDIA CORPORATION
191-200 LAWRENCE RADIATION LAB LIVERMORE
201 NEVADA OPERATIONS OFFICE,LAS VEGAS
202 BTIE OAK RIDGE,MASTER
203-[illegible] BTIE OAK RIDGE SUPPLEMENT

[redacted]

[redacted]